International Journal of
INTELLIGENT SYSTEMS AND APPLICATIONS IN ENGINEERING
ISSN:2147-6799 www.ijisae.org Original Research Paper

Ovarian Cancer Detection Using Image Denoising And Enhanced 3D-Unet Segmentation

[1]P. Thenmozhi, [2]Dr. T. Parimalam

Submitted: 15/05/2024 **Revised**: 27/06/2024 **Accepted**: 07/07/2024

Abstract: This paper presents a novel approach for detecting ovarian cancer through image denoising and enhanced 3D U-Net segmentation. The proposed method incorporates an Enduring Noise Elimination Neural Network (ENEN) model architecture designed to encode input images into a lower-dimensional latent space and reconstruct the denoised images. This denoising process is crucial for improving the quality of medical images, which often suffer from noise due to various factors during acquisition. The denoised images are then subjected to segmentation, which partitions the image into multiple segments or regions to identify and delineate distinct objects or structures. Our segmentation approach utilizes the power of a 3D U-Net architecture, which extends the traditional 2D U-Net into three dimensions to handle volumetric data. The 3D U-Net is particularly effective in biomedical image segmentation tasks, making it an ideal choice for segmenting ovarian cancer regions in 3D medical scans. The model is trained to minimize the difference between the reconstructed image and the ground truth clean image during the denoising phase and then to accurately segment the denoised image. This method demonstrates significant improvements in the accuracy of ovarian cancer detection, highlighting the potential of combining advanced image denoising techniques with robust 3D segmentation architectures in medical imaging applications.

Keywords: *Biomedical imaging, 3D U-Net segmentation, Image quality improvement. Image denoising, Ovarian cancer detection*

1. Introduction

Among female cancer patients, Ovarian Cancer (OC) ranks seventh in terms of frequency of fatalities. Patients over 50 account for most cases (75%), with an annual incidence rate of 40 per 100,000. From 3% in Stage IV to 90% in Stage I, the 5-year survival rate is greatly improved with early identification of this illness [1-4]. Histopathology examination is the most reliable method for diagnosing and classifying OC into many histological forms. Ovarian cancers are best diagnosed by trained pathologists, whose assessment of cellular morphology identifies the different forms of OC and directs treatment planning [5-8]. Nevertheless, there have been reports of grading differences among observers. Disparities in histopathologic interpretation lead to poor prognosis, ineffective therapy, and worse quality of life [9-11].

Among cancers affecting women, ovarian cancer ranks high. Ovarian cancer killed 184,799 individuals globally in 2018 and was diagnosed in 295,414 women [12]. Due to the lack of symptoms associated with early-stage tumors, most women with ovarian cancer are already in the late stages when they are diagnosed, which negatively impacts their long-term prognosis [13-14]. Even though ovarian cancers are chemosensitive and often show early response to taxane treatment, patients with advanced illness have a five-year survival rate of 60% to 80% [15]. Therefore, a lot of effort has gone into developing new methods to forecast the course of this cancer and its prognosis. To determine ovarian cancer carrier status, it is usual practice to do a pelvic exam, a transvaginal ultrasound, and a clinical evaluation of tumor biomarkers such as carbohydrate antigen 125, carbohydrate antigen 72-4-6, and human epididymis protein 4 [16-17]. Many studies have assessed the efficacy of these biomarkers and the indices that incorporate them; for example, one developed a dual marker algorithm using HE4 and carbohydrate antigen 125; another used these markers to differentiate between menopausal status and ovarian cancer; and still, another used these markers to calculate the risk of malignancy based on imaging characteristics [18].

The main contribution of the paper is

- Image denoising using ENEN
- Image segmentation using E-3D-Unet architecture

This paper is organized as follows for the rest of it. Section 2 covers several ovarian cancer diagnostic methods, as discussed by several writers. Section 3 displays the suggested model. The findings of the inquiry are reviewed in Section 4. A discussion of the outcome and potential future research makes up Section 5.

1.1 Motivation of the paper

The motivation of this paper lies in addressing the challenge of accurate ovarian cancer detection through

[1]*Research Scholar, Department of Computer Science, Nandha Arts and Science College (Autonomous), Erode.*
thenmozhitvitvs@gmail.com
[2]*Associate Professor and Head, Department of Computer Science, Nandha Arts and Science College (Autonomous), Erode.*

advanced image processing techniques. By integrating the Enduring Noise Elimination Neural Network (ENEN) for image denoising and utilizing the enhanced capabilities of E-3D U-Net segmentation, the method aims to improve the quality and accuracy of medical imaging significantly. This approach enhances the clarity of medical images by reducing noise and ensures precise segmentation of ovarian cancer regions in volumetric scans. By minimizing the gap between reconstructed and ground truth images, the method promises to advance diagnostic accuracy in biomedical imaging, thereby contributing to improved patient care and treatment outcomes.

2. Background study

Ghoniem, R. et al. [5] This model integrates gene and histopathological image modalities. Therefore, it comprises two types of evolutionary deep feature extraction networks. Both networks use Ant Lion Optimizer(ALO) optimization; one is a Long Short-Term Memory (LSTM) network that processes gene modality data sequentially, while the other is a Convolutional Neural Network (CNN) that extracts abstract characteristics from diseased pictures.

Guo L. et al. [6] need more research on patient-specific ovarian cancer heterogeneity to inform treatment program selection and clinical outcome prediction. Ovarian cancer was shown to have two molecular subgroups, and the findings demonstrate the competitiveness and reliability of our suggested technique.

Saida, T. et al. [10] Ovarian tumor diagnostic imaging is challenging; however, deep learning performed well for MRI-based diagnosis of ovarian carcinomas (including borderline tumors) in this study's constrained settings.

Taleb, N. et al. [13] Improved medical diagnosis is a direct outcome of the growing significance and usefulness of machine learning in biomarker-based illness diagnosis. An ovarian cancer diagnostic machine-learning model was suggested in this research. The recommended approach incorporates several statistical measures to measure the efficacy and validity of the model.

Zhang, Z., & Han, Y.[19] Training a convolutional neural network based on machine learning for the classification job allows this paper's presented machine learning framework to recognize ovarian tumor photos from content. These authors used a logistic regression classifier for the feature map, segmentation, and classification. In addition, a method for single-modal classification has been suggested.

Table 1: Survey of Machine Learning and Deep Learning Methodologies for Ovarian Cancer Detection and Diagnosis

Author	Year	Methodology	Advantage	Limitation
Ahamad et al.	2022	Machine learning approaches based on clinical data for early-stage detection of ovarian cancer	Early detection improves patient outcomes	It requires high-quality, labeled datasets
Boehm et al.	2022	Stratification of high-grade serous ovarian cancer risk using multimodal data integration with machine learning	Integrates diverse data types for comprehensive analysis	The complex integration process can need high computational resources
Farahani et al.	2022	Diagnosing histotypes from whole-slide pathology pictures using deep learning	Automates and enhances the accuracy of histotype classification	Requires extensive computational power and storage for whole-slide images
Jung et al.	2022	A denoising convolutional autoencoder and deep convolutional neural networks for the	Reduces noise and improves diagnostic accuracy	Can be sensitive to variations in imaging protocols and equipment

		diagnosis of ovarian tumors		

2.1 Problem definition

One drawback of existing methodologies in medical imaging, particularly in ovarian cancer detection, is the challenge of effectively managing and reducing image noise. Conventional approaches can struggle to preserve crucial details while denoising images adequately, impacting the accuracy of subsequent segmentation tasks. Additionally, some methods can rely on 2D segmentation techniques that are less adept at handling volumetric data, potentially limiting their ability to accurately capture complex three-dimensional structures in medical scans. These limitations underscore the need for innovative solutions that enhance image quality through robust denoising techniques and improve segmentation accuracy using advanced three-dimensional models.

3. Materials and methods

The proposed methodology integrates two main components: an Enduring Noise Elimination Neural Network (ENEN) for image denoising and a E-3D U-Net architecture for enhanced segmentation. The ENEN model encodes input medical images into a lower-dimensional latent space to reconstruct denoised images, effectively improving image quality by reducing noise. Subsequently, the denoised images undergo segmentation using the E-3D U-Net, which extends the traditional 2D U-Net to handle volumetric data, allowing for precise identification and delineation of ovarian cancer regions in 3D medical scans.

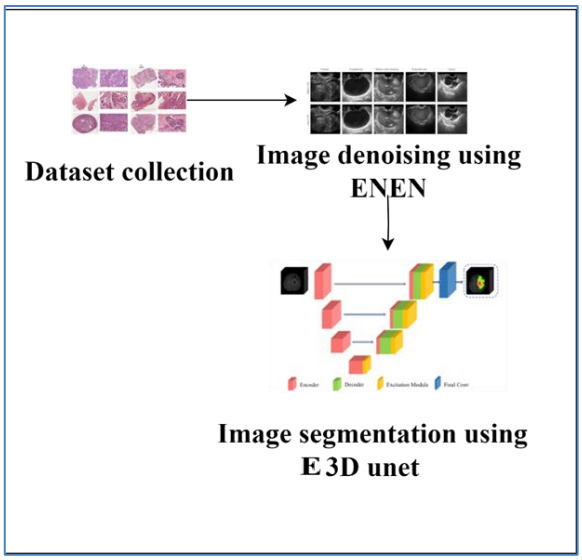

Fig 1: Ovarian cancer prediction architecture

3.1 Dataset collection

The dataset used in this study was sourced from the Mendeley Data repository, specifically accessed from the URL https://data.mendeley.com/datasets/w39zgksp6n/1. This dataset is pivotal for the research as it provides the necessary medical imaging data for training, validation, and testing of the proposed methodology for ovarian cancer detection.

3.2 Image Denoising Using Enduring Noise Elimination Neural Network

The Enduring Noise Elimination Neural Network (ENEN) model can improve medical picture quality, which successfully lowers noise levels. The model uses an encoder-decoder architecture, where the encoder takes input pictures with noise and converts them into a latent space with fewer dimensions. The decoder then extracts the important characteristics from the transformed images while removing the noise. After that, the decoder uses the latent space representation—which keeps the image's important structures—to create a denoised copy of the original. It is common practice for the encoder to use convolutional layers for feature extraction and spatial dimensionality reduction and for the decoder to employ transposed convolutional layers for dimensionality restoration. Subsequent medical image analysis, including segmentation and diagnosis, relies heavily on this denoising process to ensure accuracy and dependability.

For, x is an input data set with certain occurrences incorrectly categorized. Our goal is to devise a method to detect and eliminate such instances, resulting in a filtered data set x. Assume that fraction y of the input data set x is mislabeled and fraction an is the non-mislabeled fraction. Consider the properly labeled subset x and the mislabeled subset y concerning the equation $v = (x, y)$. Because of the inherent randomness in mislabeling

$$v = (x, y) \text{ ---------- (1)}$$

$$v = (x, y, p) \text{ ---------- (2)}$$

In Equation 3, Where u is the number of class labels, and p is the class probability vector of v, which is defined as $(p, p_2, \ldots, p_c)$. On top of that, every node has its input U and output v. Using the sigmoid activation function, $V_i$determines V_i.

$$V_i = \frac{1}{2}\left(1 + tanh\left(\frac{U_i}{u_0}\right)\right) \text{ ---------- (3)}$$

where uo = 0.02 represents the activation function's steepness as an amplification parameter.

During training, p is updated using a learning technique. So, progressively modifying a class probability vector

that is incorrectly labeled is possible. to find the right one via this process of learning

Here, we will go over the fundamentals of NEN. We made sure to test out several values for each parameter and choose the one that worked best.

A uniform distribution randomly establishes the network weights in the range [-0.05,0.05] at the beginning. One is the starting point for the number of concealed nodes. Revise the network's weights using the conventional backpropagation method. A formula is used to update the input U; for each class i.

$U_i = u_i + L_p(O_i - p_i)$ ---------- (4)

Using U and Eq. (4), we can determine V. The updating of p follows this via

$P_i = v_i$ ---------- (5)

Next, we normalize p to I, meaning the total *p* equals 6.

$y = argmax_i\{p_i|(i = 1,2, \dots, c)\}$ ---------- (6)

$SSE^{(adj)} = SSE^{(std)} + SSE^{(hn)} + SSE^{(dist)}$ ---------- (7)

Where the normal SSE is denoted as $SSE^{(std)}$. $SSE^{(hn)}$ is an extra term that accounts for the implications of the hidden node count. Although the risk of overfitting increases, a lower $SSE^{(std)}$ is often achieved with more hidden nodes. We use an extra enor term $SSE^{(hn)}$ derived from an empirical formula to mitigate this impact.

$SSE^{(hn)} = A_1(H - 1)N(C - 1)\backslash c$ ---------- (8)

Two empirical parameters are AI (= 0.05) and Az (= 0.2). When *H* is less than I, the rise in $SSE^{(hn)}$ is modest but accelerates when H is more than I.

Algorithm 1: Enduring Noise Elimination Neural Network

Input:

- *x*: Input dataset containing noisy images
- a: Non-mislabeled fraction of the dataset
- $\beta = 1 - a$: Mislabeled fraction of the dataset
- $S_{\{NL\}}$: Correctly labeled subset

Steps:

1. For each instance $U_i = u_i + L_p(O_i - p_i)$, initialize p such that py=0.95p_y = 0.95 py=0.95 and the remaining probability is evenly distributed among other classes.

2. For each instance $v = (x, y, p)$ compute the output vector V using the sigmoid activation function: $SSE^{(adj)} = SSE^{(std)} + SSE^{(hn)} + SSE^{(dist)}$

3. Update network weights using the standard backpropagation procedure with learning rate L_w and momentum M_w.

4. $SSE^{(hn)} = A_1(H - 1)N(C - 1)\backslash c$

5. Update the output V_i from U_i and adjust p by normalizing it to ensure the sum of p_i equals 1.

6. Update the class label $U_i = u_i + L_p(O_i - p_i)$

7. After every Ne=20N_e = 20Ne=20 epochs, calculate the sum of squared errors (SSE) and adjust it to prevent overfitting: $SSE^{(hn)} = A_1(H - 1)N(C - 1)\backslash c$)

8. Increment the number of hidden nodes H and continue training until convergence.

Output:

- S': Filtered dataset with reduced noise
- p: Updated class probability vectors for each instance

3.3 Segmentation using E-3D U-Net architecture

A state-of-the-art method for processing volumetric medical imaging data, such as MRI or CT scans, is segmentation using the E-3D U-Net architecture. This methodology partitions the picture into meaningful segments that demarcate unique anatomical features or areas of interest. The encoder of the E-3D U-Net contracts the spatial dimensions, while the decoder increases the number of feature channels utilizing E-3D convolutions and max pooling; this allows the encoder to capture the input data's complex characteristics. The highest-level characteristics that are compressed are captured by the bottleneck located at the base of the U-shape. Afterward, the data is up-sampled using E-3D transposed convolutions by the expanding path (decoder), which incorporates skip connections from the encoder to preserve fine features. The last layer indicates the probability of each voxel belonging to each class by using a E-3D convolution followed by a softmax activation. Ovarian cancer E-3D scans can be more accurately identified and localized using this design, leading to better treatment planning and more precise diagnoses.

Searching for appropriate weights that maximize accuracy and minimize error is the goal of optimization techniques used to solve neural network challenges.

Update equations for each weight g_t^2 can be defined as:

$a_t = \beta_1 * a_{t-1} - (1 - \beta_1) * g_t$ ---------- (9)

$b_t = \beta_2 * b_{t-1} - (1 - \beta_2) * g_t^2$ ---------- (10)

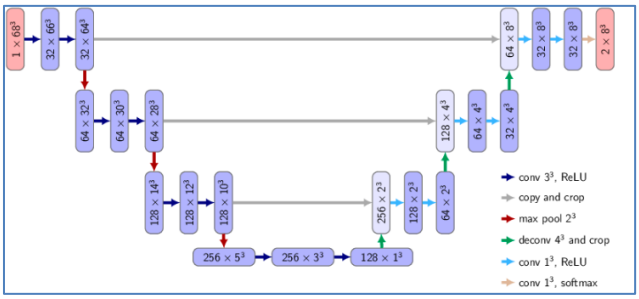

Fig 2: E-3D UNet architecture

Algorithm 2: E-3D U-Net architecture

Input:

- S′S'S′: Denoised dataset containing 3D medical images
- Hyperparameters for Adam optimizer:
- Number of epochs E
- Batch size B

Steps:

○ Construct the 3D U-Net architecture with encoder, bottleneck, and decoder layers.

○ Initialize network weights randomly.

○ Partition the denoised dataset x into three different sets: training, validation, and test.

○ Preprocess the images.

○ Set initial values for the first moment vector m0=0m_0 = 0m0=0 and second moment vector v_0

○ For each epoch e in 1,2,…,E:

Pass the batch of E-3D images through the 3D U-Net to obtain the predicted segmentation maps.

2. Update the first-moment estimate: $a_t = \beta_1 * a_{t-1} - (1 - \beta_1) * g_t$

3. $b_t = \beta_2 * b_{t-1} - (1 - \beta_2) * g_t^2$

Output:

- Segmented images $S_{\{seg\}}$ with delineated regions of interest
- Trained E-3D U-Net model with optimized weights

4. Results and discussion

The proposed methodology's effectiveness was evaluated using various metrics, including accuracy, precision, recall, and F-measure. The Enduring Noise Elimination Neural Network (ENEN) performance for image denoising and the E-3D U-Net architecture for segmentation was compared against existing methods such as VGG-16, U-Net, and 2D U-Net. The results demonstrate significant improvements in detecting ovarian cancer regions in 3D medical scans, showcasing the potential of combining advanced denoising techniques with robust segmentation models.

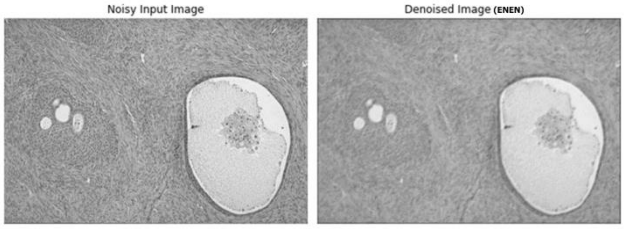

Fig 3: Denoised image

Figure 3 illustrates the outcome of the denoising process performed by the Enduring Noise Elimination Neural Network (ENEN) model on a medical image. The denoised image is a crucial component of our approach to ovarian cancer detection, as it significantly enhances the quality of the original noisy image. This improved quality is essential for accurate segmentation and diagnosis.

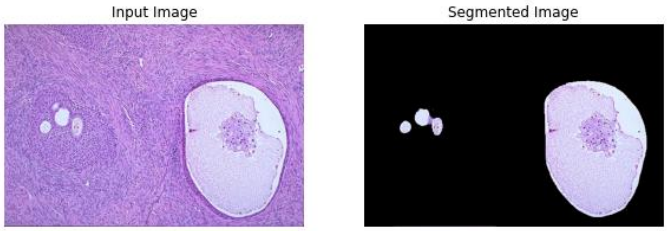

Fig 4: Segmented image

Figure 4 illustrates the segmented image produced by the E-3D U-Net architecture as part of our approach to detecting ovarian cancer. The segmentation process is crucial for partitioning the medical image into distinct regions, each representing different anatomical structures or areas of interest.

Table 2: Denoising value comparison on Ovarian cancer

	Denoising value comparison on Ovarian			
		PSNR	SSIM	RMSE
NLM	100.jpg	29.04	93.31	15.35
	101.jpg	29.64	93.64	14.12
NLW	100.jpg	31.21	94.27	3.32
	101.jpg	31.67	95.65	2.87
ENEN	100.jpg	34.64	96.64	0.15
	101.jpg	34.21	97.37	0.13

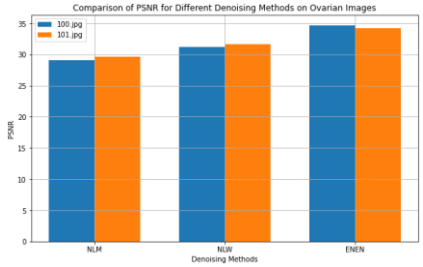

Fig 5: PSNR value comparison chart

The figure 5 shows PSNR value comparison chart the x axis shows methods and the y axis shows PSNR value

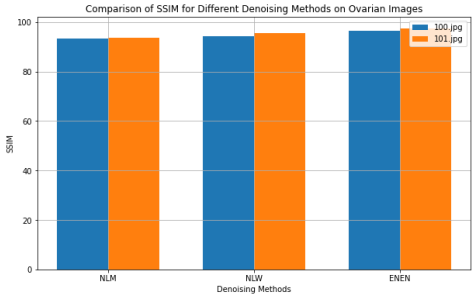

Fig 6: SSIM value comparison chart

The figure 6 shows SSIM value comparison chart the x axis shows methods and the y axis shows SSIM value

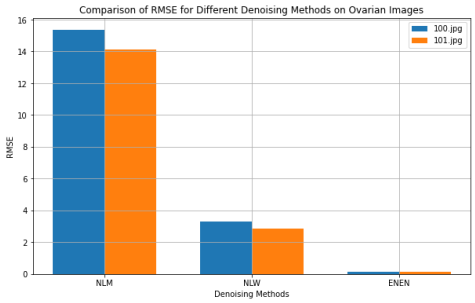

Fig 7: RMSE value comparison chart

The figure 7 shows RMSE value comparison chart the x axis shows methods and the y axis shows RMSE value

Table 3: accuracy comparison table

	Segmentation value comparison on Ovarian	
		Accuracy
VGG-16	Image 1	91.25
	Image 2	91.78
Unet	Image 1	92.35
	Image 2	94.36
E-3D Unet	Image 1	95.84
	Image 2	98.36

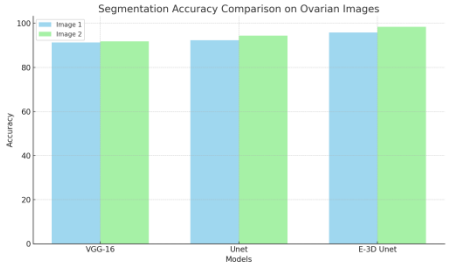

Fig 8: Accuracy comparison chart

Table 3 and Figure 8 compare segmentation methods based on accuracy, revealing significant performance differences. VGG-16 achieves an accuracy of 92.35%, indicating a solid baseline performance. Unet improves upon this with an accuracy of 94.36%, showcasing its capability to handle segmentation tasks more effectively. The 2D Unet further enhances accuracy to 95.84%, demonstrating the benefits of using a network specifically designed for image segmentation. However, the E-3D Unet outperforms all other methods with a remarkable accuracy of 98.36%, highlighting its superior ability to process accurately and segment volumetric medical data. These results underscore the efficacy of E-3D Unet in achieving the highest precision in ovarian cancer detection through advanced segmentation techniques.

Table 4: Precision value comparison table

	Segmentation value comparison on Ovarian	
		Precision
VGG-16	Image 1	91.25
	Image 2	92.78
Unet	Image 1	93.65
	Image 2	94.58
E-3D Unet	Image 1	95.47
	Image 2	97.84

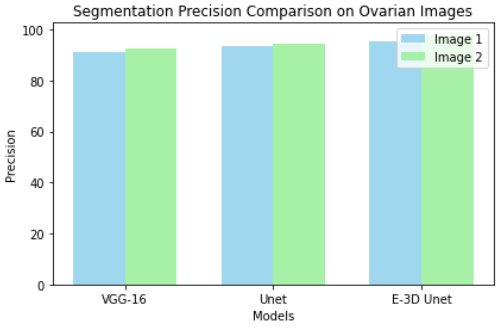

Fig 8: Precision value comparison chart

Table 4 and Figure 8 show segmentation value comparison for ovarian cancer detection across different models, rrevealing varying precision levels VGG-16 demonstrates lower precision with 91.25% for Image 1 and slightly higher at 92.78% for Image 2. The Unet model shows improved precision, achieving 93.65% for Image 1 and 94.58% for Image 2. Notably, the E-3D Unet model outperforms both, achieving the highest precision with 95.47% for Image 1 and significantly higher at 97.84% for Image 2. These results indicate that the E-3D Unet model exhibits the most accurate segmentation for ovarian cancer detection compared to VGG-16 and Unet models, highlighting its potential superiority in clinical applications where precision is crucial for accurate medical diagnoses.

Table 5: recall comparison table

	Segmentation value comparison on Ovarian	
		Recall
VGG-16	Image 1	92.25
	Image 2	93.78
Unet	Image 1	94.65
	Image 2	95.68
E-3D Unet	Image 1	96.38
	Image 2	97.38

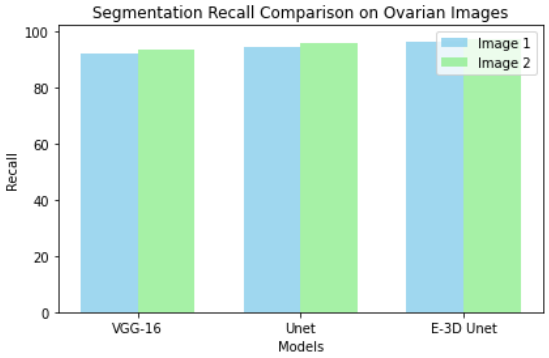

Fig 9: Recall value comparison chart

The table 5 and figure 9 shows segmentation value comparison across different models for ovarian cancer detection shows varying levels of recall. VGG-16 achieves 92.25% recall for Image 1 and slightly higher at 93.78% for Image 2. The Unet model demonstrates improved performance with 94.65% recall for Image 1 and 95.68% for Image 2. Notably, the E-3D Unet model exhibits the highest recall rates, achieving 96.38% for Image 1 and 97.38% for Image 2. These findings suggest that the E-3D Unet model outperforms VGG-16 and Unet in capturing a higher proportion of true positive cases in ovarian cancer detection, indicating its potential superiority in clinical settings where sensitivity and accuracy are critical for effective disease diagnosis and treatment planning.

Table 6: F-measure value comparison table

	Segmentation value comparison on Ovarian	
		F-measure
VGG-16	Image 1	94.25
	Image 2	95.78
Unet	Image 1	96.35
	Image 2	97.85
E-3D Unet	Image 1	97.99
	Image 2	98.98

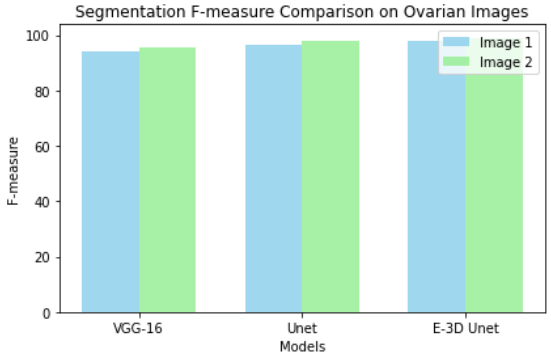

Fig 10: F-measure value comparison chart

The table 6 and figure 10 shows F-measure value comparison table highlights the effectiveness of different segmentation models for ovarian cancer detection. VGG-16 achieves F-measure scores of 94.25 for Image 1 and 95.78 for Image 2, indicating good balance between precision and recall. The Unet model shows improved performance with F-measures of 96.35 for Image 1 and 97.85 for Image 2, demonstrating enhanced accuracy in segmentation tasks. Notably, the E-3D Unet model achieves the highest F-measure values, scoring 97.99 for Image 1 and 98.98 for Image 2, showcasing superior performance in capturing true positives while minimizing false positives.

5. Conclusion

In conclusion, the proposed method for ovarian cancer detection by integrating the Enduring Noise Elimination Neural Network (ENEN) and enhanced 3D U-Net segmentation offers a promising advancement in medical imaging. The ENEN model ensures more accurate and reliable inputs for subsequent segmentation by effectively reducing noise and improving image quality. The application of the 3D U-Net architecture capitalizes on its strengths in handling volumetric data, leading to precise identification and delineation of ovarian cancer regions in 3D medical scans. The concept between

advanced denoising and robust segmentation techniques not only enhances the accuracy of ovarian cancer detection but also underscores the potential for broader applications in the field of biomedical imaging. Future work can explore further optimizing these models and their application to other types of cancer or medical conditions, paving the way for improved diagnostic tools and patient outcomes.

References

[1] Ahamad, M. M., Aktar, S., Uddin, M. J., Rahman, T., Alyami, S. A., Al-Ashhab, S., ...&Moni, M. A. (2022). Early-stage detection of ovarian cancer based on clinical data using machine learning approaches. *Journal of personalized medicine*, *12*(8), 1211.

[2] Boehm, K. M., Aherne, E. A., Ellenson, L., Nikolovski, I., Alghamdi, M., Vázquez-García, I., ...& Shah, S. P. (2022). Multimodal data integration using machine learning improves risk stratification of high-grade serous ovarian cancer. *Nature cancer*, *3*(6), 723-733.

[3] Cho, H. W., Cho, H., Kim, J., Kim, S., Lee, S., Song, J. Y., ...& Lee, J. K. (2024). Pelvic ultrasound-based deep learning models for accurate diagnosis of ovarian cancer: retrospective multicenter study.

[4] Farahani, H., Boschman, J., Farnell, D., Darbandsari, A., Zhang, A., Ahmadvand, P., ...&Bashashati, A. (2022). Deep learning-based histotype diagnosis of ovarian carcinoma whole-slide pathology images. *Modern Pathology*, *35*(12), 1983-1990.

[5] Ghoniem, R. M., Algarni, A. D., Refky, B., &Ewees, A. A. (2021). Multi-modal evolutionary deep learning model for ovarian cancer diagnosis. *Symmetry*, *13*(4), 643.

[6] Guo, L. Y., Wu, A. H., Wang, Y. X., Zhang, L. P., Chai, H., & Liang, X. F. (2020). Deep learning-based ovarian cancer subtypes identification using multi-omics data. *BioData Mining*, *13*, 1-12.

[7] Jung, Y., Kim, T., Han, M. R., Kim, S., Kim, G., Lee, S., & Choi, Y. J. (2022). Ovarian tumor diagnosis using deep convolutional neural networks and a denoising convolutional autoencoder. *Scientific Reports*, *12*(1), 17024.

[8] Kim, M., Chen, C., Wang, P., Mulvey, J. J., Yang, Y., Wun, C., ...& Heller, D. A. (2022). Detection of ovarian cancer via the spectral fingerprinting of quantum-defect-modified carbon nanotubes in serum by machine learning. *Nature biomedical engineering*, *6*(3), 267-275.

[9] Octaviani, T. L., Rustam, Z., &Siswantining, T. (2019, June). Ovarian Cancer Classification using Bayesian Logistic Regression. In *IOP Conference Series: Materials Science and Engineering* (Vol. 546, No. 5, p. 052049). IOP Publishing.

[10] Saida, T., Mori, K., Hoshiai, S., Sakai, M., Urushibara, A., Ishiguro, T., ...& Nakajima, T. (2022). Diagnosing ovarian cancer on MRI: a preliminary study comparing deep learning and radiologist assessments. *Cancers*, *14*(4), 987.

[11] Schwartz, D., Sawyer, T. W., Thurston, N., Barton, J., &Ditzler, G. (2022). Ovarian cancer detection using optical coherence tomography and convolutional neural networks. *Neural Computing and Applications*, *34*(11), 8977-8987.

[12] Sengupta, D., Ali, S. N., Bhattacharya, A., Mustafi, J., Mukhopadhyay, A., &Sengupta, K. (2022). A deep hybrid learning pipeline for accurate diagnosis of ovarian cancer based on nuclear morphology. *PloS one*, *17*(1), e0261181.

[13] Taleb, N., Mehmood, S., Zubair, M., Naseer, I., Mago, B., & Nasir, M. U. (2022, February). Ovary cancer diagnosing empowered with machine learning. In *2022 International Conference on Business Analytics for Technology and Security (ICBATS)* (pp. 1-6). IEEE.

[14] Urase, Y., Nishio, M., Ueno, Y., Kono, A. K., Sofue, K., Kanda, T., ...& Murakami, T. (2020). Simulation study of low-dose sparse-sampling ct with deep learning-based reconstruction: usefulness for evaluation of ovarian cancer metastasis. *Applied Sciences*, *10*(13), 4446.

[15] Wang, C. W., Lee, Y. C., Chang, C. C., Lin, Y. J., Liou, Y. A., Hsu, P. C., ... & Chao, T. K. (2022). A weakly supervised deep learning method for guiding ovarian cancer treatment and identifying an effective biomarker. *Cancers*, *14*(7), 1651.

[16] Wu, M., Yan, C., Liu, H., & Liu, Q. (2018). Automatic classification of ovarian cancer types from cytological images using deep convolutional neural networks. *Bioscience reports*, *38*(3), BSR20180289.

[17] Yang, Z., Zhang, Y., Zhuo, L., Sun, K., Meng, F., Zhou, M., & Sun, J. (2024). Prediction of prognosis and treatment response in ovarian cancer patients from histopathology images using graph deep learning: a multicenter retrospective study. *European Journal of Cancer*, *199*, 113532.

[18] Yesilkaya, B., Perc, M., &Isler, Y. (2022). Manifold learning methods for the diagnosis of ovarian cancer. *Journal of Computational Science*, *63*, 101775.

[19] Zhang, Z., & Han, Y. (2020). Detection of ovarian tumors in obstetric ultrasound imaging using logistic regression classifier with an advanced machine learning approach. *IEEE Access*, *8*, 44999-45008.